Chem. Eur. J. 2019, 25, 8061 – 8069 DOI: 10.1002/chem.201900961

Cyclic(Alkyl)(Amino)Carbene (CAAC)-supported Zn alkyls: synthesis, structure and reactivity in hydrosilylation catalysis

Jean-Charles Bruyere,[a] David Specklin,[a] Christophe Gourlaouen,[a] Rosita Lapenta,[a,b] Luis F. Veiros,[c] Alfonso Grassi,[b] Stefano Milione,[b] Laurent Ruhlmann,[a] Corinne Boudon,[a] and Samuel Dagorne*[a]

Abstract: The reaction of Zn(II) dialkyl species $ZnMe_2$ with a Cyclic(Alkyl)(Amino)Carbene, 1-[2,6-bis(1-methylethyl)phenyl]-3,3,5,5-tetramethyl-2-pyrrolidinylidene (CAAC, **1**), was studied and extended to the preparation of CAAC-supported Zn(II) Lewis acidic organocations. CAAC adduct of $ZnMe_2$ (**2**), formed from a 1/1 mixture of **1** and $ZnMe_2$, is unstable at room temperature and readily undergoes a CAAC carbene insertion into the Zn–Me bond to produce the ZnX_2-type species (CAAC–Me)Zn–Me (**3**), as deduced from NMR data and the solid state structure of **3**. Insertion product **3** is also unstable at room temperature and decomposes to 1-(2,6-diisopropylphenyl)- 2,2,4,4-tetramethyl-5-methylenepyrrolidine (**4**) and 1-(2,6- diisopropylphenyl)-5-ethylidene-2,2,4,4-tetramethylpyrrolidine (**4'**) as major organic products, along with Zn metal, $ZnMe_2$ and CH_4. Despite its limited stability, adduct **2** may be cleanly ionized to robust two- coordinate (CAAC)Zn–Me^+ cation (**5**$^+$) and derived into (CAAC)Zn–C F $^+$ (**7**$^+$), both isolated as B(C F) $^-$ salts, reflecting the ability of CAAC for the stabilization of reactive $[Zn–Me]^+$ and $[Zn–C_6F_5]^+$ moieties. Due to the lability of the CAAC–$ZnMe_2$ bond, the formation of *bis*-CAAC adduct $(CAAC)_2Zn–Me^+$ cation (**6**$^+$) was also observed and salt [**6**][$B(C_6F_5)_4$] was structurally characterized. As estimated from experimental and calculations data, cations **5**$^+$ and **7**$^+$ are highly Lewis acidic species and the stronger Lewis acid **7**$^+$ effectively mediates alkene, alkyne and CO_2 hydrosilylation catalysis. All supporting data hints at Lewis-acid-type activation/functionalization processes.

[a] J.-C. Bruyere, Dr. D. Specklin, Dr. C. Gourlaouen, R. Lapenta, Pr. L. Ruhlmann, Pr. C. Boudon, Dr. S. Dagorne
Institut de Chimie (UMR CNRS 7177)
Université de Strasbourg
4 rue Blaise Pascal, 67000 Strasbourg (France)
E-mail: dagorne@unistra.fr

[b] R. Lapenta, Pr. A. Grassi, Dr. S. Milione.
Dipartimento di Chimica eBiologia "Adolfo Zambelli"
Università degli Studi di Salerno
Via Giovanni Paolo II, 84084 Fisciano (SA) (Italy)

[c] Pr. L. F. Veiros
Centro de Química Estrutural, Instituto Superior Técnico
Universidade de Lisboa,
Av. Rovisco Pais No. 1, 1049-001 Lisboa (Portugal)

Supporting information for this article is given via a link at the end of the document.

Introduction

N-heterocyclic carbenes (NHCs) are ubiquitous ligandsin coordination chemistry for the stabilization of various metal/heteroatom centers, which has led to significant progress in metal-catalyzed reactions and fundamental organometallic reactivity.[1] NHC coordination has attracted considerable attention for the stabilization of unprecedented organometallic/inorganic entities both in main group and transition metal chemistry.[2] Cyclic(Alkyl)(amino)carbenes (CAACs) are now emerging as promising carbene ligands that may well complement and even outperform NHCs due to their specificelectronic properties: *i.e.* an enhanced σ-donation and a stronger π-accepting ability *vs.* NHCs.[3] Recent studies on CAAC coordination demonstrated their effective ability to stabilize a number of low-coordinate transition metal species, most notably CAAC-supported Au(I), Pd(II), Rh(I) and Ni(II) species.[3,4,5] In main group chemistry, several unusual structural motifs were also recently characterized thanks to the specific electronic properties of CAAC ligands, noticeably including a CAAC-supported formally B(I) compound,[6] CAAC-stabilized radicals and diradicals,[7] as well as bis(CAAC) adducts of phosphorus arising from the fragmentation of P_4 by free CAAC.[8] The activation and functionalization of E–H or E–E bonds (E = B, Si, Al; primarily in boranes, diboron species and silanes) by CAAC ligands, are also documented and typically lead to the formal insertion of the CAAC carbene atom into the E–H or E–E bond.[9]

Besides fundamental reactivity, the use of CAAC-supported metal complexes is also emerging in homogeneous catalysis, thus far essentially with carbophilic metal centers.[5] Most notably, CAAC-Au(I) species were shown to be extremely robust catalysts (even under harsh conditions) for the hydroamination (with NH_3 or $NH_2–NH_2$) of alkynes and allenes, reflecting the exceptional stability of the CAAC-Au(I) moiety in such catalysts.[5,10] Also noteworthy, the use of a CAAC-supported Rh(I) catalyst (instead of a NHC analogue) was found to be crucial for high selectivity and activity in aromatic ketones hydrogenation catalysis, illustrating the interest of CAAC-based metal species in catalysis.[11]

Due to their attractive features, including a cheap and non-toxic metal source and an enhanced stability thanks to NHC coordination, NHC-Zn(II) adducts are currently attracting interest, in particular for zinc-mediated catalytic processes.[12] This includes the recent development of Zn-NHC catalysts in imine hydrogenation, CO_2 reductive amination, CO_2 hydrosilylation, alkene/alkyne hydrosilylation, allylic alkylation and cyclic

esters/carbonates polymerization.[13] NHC strong σ-donation also provides enhanced stability to Lewis acidic Zn(II) organocations, allowing the recent characterization of unprecedented two-coordinate Zn(II)–alkyl cations.[12,14,15] Due to their even stronger σ donor character, CAAC ligands stand as potential candidates for additional stability at Zn(II), an attractive feature for further fundamental developments of organozinc chemistry and related catalytic applications.[16] Yet, contrasting with the recent interest in NHC-Zn derivatives, examples of CAAC-supported Zn(II) species are restricted, to our knowledge, to a report by Roesky, Frenking and Dittrich on the reduction of adduct (CAAC)$ZnCl_2$ to afford either a singlet biradicaloid Zn(II) species or the ZnX_2-type species $(CAAC–H)_2Zn$.[17] More generally, the fundamental reactivity and the suitability in catalysis of CAAC complexes of electron-deficient, Lewis acidic and oxophilic metals centers remain to be explored.

We herein report on the reactivity of free CAAC **1** (Scheme 1) with a simple Zn(II) dialkyl precursor such as $ZnMe_2$ and subsequent derivatization chemistry to access CAAC-supported Zn(II) organocations. As detailed below, combining CAAC **1** with $ZnMe_2$ may be the source of unexpected reactivity but also afford robust (CAAC)Zn–R^+ and $(CAAC)_2Zn–R^+$ cations, some of which being exploited in hydrosilylation catalysis. The structural features and catalytic performance of such cations are also compared to those of NHC-Zn analogues.[14b] Experimental data are also supported, whenever possible and appropriate, with DFT calculations.

Results and Discussion

Reactivity of CAAC 1 with $ZnMe_2$. To access adduct (CAAC)$ZnMe_2$ (**2**, Scheme 1), CAAC **1**, synthesized according to a literature procedure,[3a] was reacted with 1 equiv of $ZnMe_2$ under reaction conditions typically used to prepare (NHC)ZnR_2 (R = alkyl) species (toluene or pentane, -35 °C to RT, overnight). However, such conditions only led to decomposition products, among which CAAC-derived organics **4** and **4'** (94% conv. to a 2/1 **4**/**4'** mixture, Scheme 1) and Zn(0) metal (precipitation from the reaction medium) were identified as major products, hence indicating the instability of adduct (CAAC)$ZnMe_2$ (**2**) at room temperature. The molecular structures of **4** and **4'** were unambiguously determined through 1D and 2D homo-/hetero-nuclear NMR studies and confirmed by HRMS data (Figures S10-S15, SI). Powder X-ray diffraction data for the metallic residue agree with the formation of Zn(0) (Figure S16, SI).[18] To gain insight on the reaction between **1** and $ZnMe_2$, low temperature ^1H and ^{13}C NMR monitoring studies of a 1/1 **1**/$ZnMe_2$ mixture (toluene d^8) were performed and indicated the immediate and quantitative formation of CAAC adduct **2** at -40 °C (Figures S1 and S2, SI). In particular, the ^{13}C NMR spectrum of **2** at -40 °C displays a significantly upfield $C_{carbene}$ signal (δ 267.6 ppm) *vs.* that of free CAAC **1** (δ 304.3 ppm), consistent with CAAC coordination to Zn(II). While stable for hours at -40 °C, adduct **2** quickly rearranges at room temperature to species (CAAC–Me)ZnMe (**3**, 72% conversion after 45 min at RT, Scheme 1; Figure S3, SI), thus formally resulting from the insertion of CAAC **1** carbene atom into a Zn–Me bond of $ZnMe_2$. The identity of species **3** in solution was determined through various 1D and 2D NMR experiments (COSY, NOESY, HMBC, HSQC) performed at -40 °C, all data being consistent with a C_1-symmetric species, the presence of one Zn–*Me* moiety and a (*Me*)C–Zn group (Figures S4-S9, SI). Compound **3** is also unstable at room temperature and slowly decomposes over the course of several hours to a mixture of products (organics **4** and **4'** in a 2/1 ratio, free $ZnMe_2$ and CH_4), as deduced from NMR data.

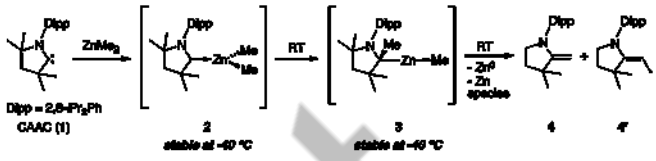

Scheme 1. Reactivity of carbene CAAC **1** with $ZnMe_2$.

Despite the limited stability of CAAC insertion product **3**, its molecular structure could be unambiguously confirmed through X-ray diffraction studies (crystals grown from saturated pentane solution of a 1/1 **1**/$ZnMe_2$ mixture at -40 °C). As depicted in Figure 1, species **3** indeed consists of ZnX_2-type species with a two-coordinate *sp*-hybridized Zn(II) center (C(1)–Zn(1)–C(22) = 176.8(2) °) stabilized by $[CAAC–Me]^-$ and Me^- groups as X-type ligands. The Zn–$C_{CAAC-Me}$ bond distance (2.017(4) Å) is longer than that of the Zn–Me bond (1.957(6) Å).

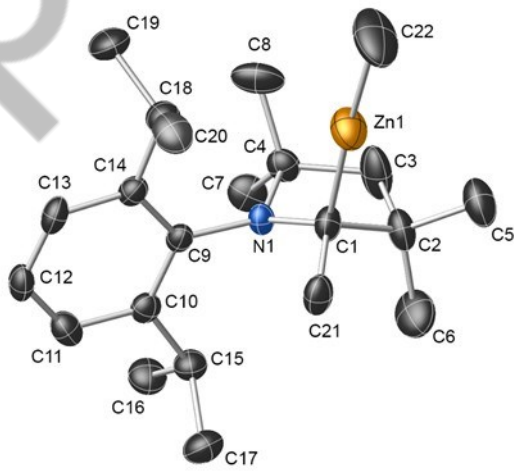

Figure 1. Molecular structure of species (CAAC-Me)Zn–Me (**3**, ORTEP plot with thermal ellipsoids shown at the 30% probability level). Hydrogen atoms are omitted for clarity. Selected distances (Å) and angles (°): Zn(1)–C(1) = 2.017(4), Zn(1)-C(22) = 1.957(6), C(1)–N(1) = 1.470(5), C(1)–C(21) = 1.507(6), C(1)–Zn(1)–C(22) = 176.8(2).

To further rationalize the formation of **3** from **1** and $ZnMe_2$, DFT calculations were performed (B3LYP/6-31+G** with Grimme's GD3 corrections, Figure 2; Figures S35-38, SI). From model CAAC **I** and $ZnMe_2$, the formation of model adduct **II** (ΔG = -3.8 $kcal.mol^{-1}$) is only slightly exergonic, thus suggesting a rather labile (CAAC)$ZnMe_2$ adduct. Adduct **II** may then undergo an

intramolecular Me^- transfer from the Zn(II) center to the Zn–C_{CAAC} atom through transition state **TS-II-III** (ΔG = 15.8 kcal.mol^{-1}) to afford the thermodynamically favored (CAAC–Me)Zn–Me product **III** (ΔG = -7.4 kcal.mol^{-1}). The formation of **III** from **I** and $ZnMe_2$ is thus exergonic and proceeds through a low energy barrier ($\Delta\Delta G$ = 19.6 kcal.mol^{-1} from adduct **II**), in agreement with experimental observations. From model **III** and despite several mechanisms probed by DFT, no reasonable pathway accounting for the formation of decomposition products **4**, **4'**, CH_4 and $ZnMe_2$ could be computed.

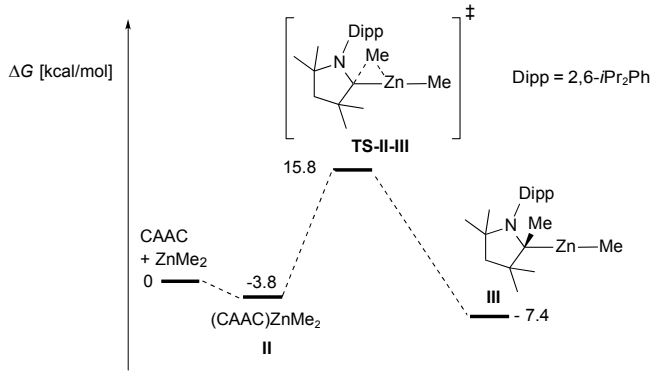

Figure 2. DFT-computed (B3LYP/6-31+G**, toluene) reaction profile for the formation of model **III** from CAAC and $ZnMe_2$.

Overall, the ready formation of insertion product **3** from unstable CAAC adduct **2** clearly reflects the enhanced electrophilicity of the CAAC carbene atom and further illustrates the ability of CAACs to activate/functionalize various small molecules through insertion reactivity.[9] Though CAAC insertion in Zn–alkyl bonds is not documented, a related carbene insertion reactivity was recently reported upon combining ZnR_2 dialkyls with diamidocarbenes.[19]

CAAC-supported Zn–R Organocations 5^+, 6^+ and 7^+ as $B(C_6F_5)_4^-$ salts. A primary goal of the present study was the synthesis of two-coordinate Zn(II) cations of the type (CAAC)Zn–R^+ as electrophilic organometallics. Cation (CAAC)Zn–Me^+ (**5**$^+$, Scheme 2) may be readily generated by slow addition of adduct **2**, generated *in situ* at -35 °C, to 1 equiv of $[Ph_3C][B(C_6F_5)_4]$ (-35 to 0 °C, PhF, 1 h) and was isolated as a $B(C_6F_5)_4^-$ salt ([**5**][$B(C_6F_5)_4$]) in good yield (67%). In contrast, fast mixing of a 1/1 $[Ph_3C][B(C_6F_5)_4]$/**2** (-35 to 0 °C, PhF, 1 h) afforded a 1/1 mixture of the *bis*-CAAC adduct cation $(CAAC)_2Zn–Me^+$ (**6**$^+$, Scheme 2) and $ZnMe_2$, as deduced from ^{1}H NMR data. The formation of **6**$^+$ arises from a CAAC ligand re-distribution reaction presumably occurring between immediately formed cation **5**$^+$ and unreacted adduct **2**, and thus indicates the lability of the CAAC–Zn(II) bond in adduct **2**. Such carbene exchange reactions were not observed in NHC-Zn chemistry under identical experimental conditions.[14] The identity of salt [**6**][$B(C_6F_5)_4$] was confirmed by its independent synthesis by reaction of a 1/2 $[Ph_3C][B(C_6F_5)_4]$/**2** mixture, allowing its isolation in 75% yield and its molecular structure was established through XRD studies (*vide infra*).

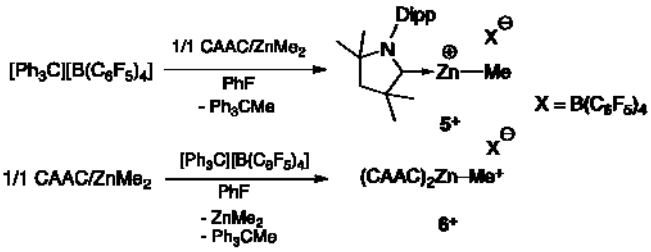

Scheme 2. Synthesis of CAAC-supported Zn organocations **5**$^+$ and **6**$^+$ as $B(C_6F_5)_4^-$ salts.

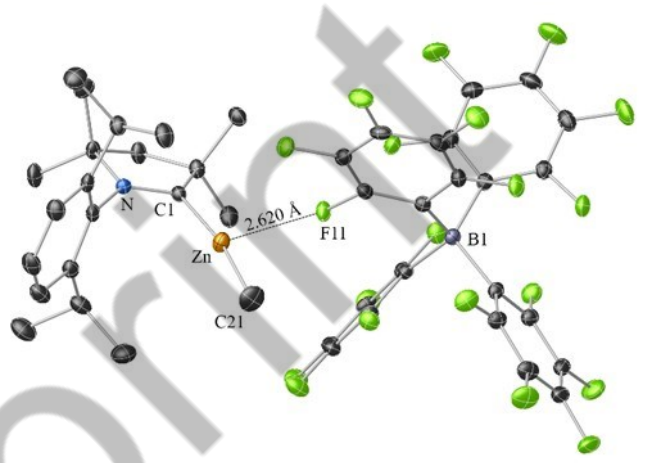

Figure 3. Molecular structure of [(CAAC)Zn–Me][$B(C_6F_5)_4$] ([**5**][$B(C_6F_5)_4$]), ORTEP plot with thermal ellipsoids shown at the 30% probability level). Hydrogen atoms are omitted and selected atoms are labelled for clarity. Selected distances (Å) and angles (°): Zn–C(1) = 1.976(3), Zn–C(21) = 1.913(4), Zn···F(11) = 2.620(3), C(1)–Zn–C(21) = 170.2(2).

Unlike its parent compound **2**, CAAC-supported Zn–Me^+ **5**$^+$ is thermally stable at ambient temperature whether in the solid state or in solution. At room temperature, it is stable for days in C_6D_5Br but decomposes within minutes in CD_2Cl_2 to unknown species. NMR data for [**5**][$B(C_6F_5)_4$] (C_6D_5Br, RT) agree with the proposed formulation, with, in particular, a ^{13}C NMR $C_{carbene}$ signal for **5**$^+$ significantly upfield shifted *vs.* that of the neutral precursor **2** (δ 231.7 and 267.6 ppm, respectively), which is in line with a more Lewis acidic Zn(II) in **5**$^+$.[20] As determined through X-ray diffraction studies, salt [**5**][$B(C_6F_5)_4$] crystallizes as discrete **5**$^+$ and $B(C_6F_5)_4^-$ ions in close contact (Figure 3) with a rather short Zn(1)···F(11) distance (2.620 Å, *i.e.* 0.2 Å shorter than the sum of the van der Waals radii for Zn and F). Cation **5**$^+$ incorporates a central two-coordinate *sp*-hydridized Zn(II) center with Zn–C_{CAAC} and Zn–Me^+ bond distances (1.976(3) and 1.913(4) Å, respectively) similar to those in (IDipp)Zn–Me^+ (1.943(2) Å and 1.895(1) Å), in line with an enhanced electrophicity at Zn(II). Unlike [**5**][$B(C_6F_5)_4$], the solid state structure of the *bis*-CAAC adduct species [**6**][$B(C_6F_5)_4$] (Figure 4) consists of fully dissociated ions with no **5**$^+$/$B(C_6F_5)_4^-$ close contacts, reflecting an greater steric hindrance at Zn(II) due to an additional CAAC ligand and a less electrophilic Zn(II) center. Cation **6**$^+$ is a three-

coordinate Zn(II) center with a distorted trigonal geometry (C(21)–Zn(1)–C(1) = 125.03(1) °). The Zn–C_{CAAC} bond distances in **6**$^+$ [2.052(3) and 2.045(3) Å] are significantly longer than in **5**$^+$ (1.976(3) Å).

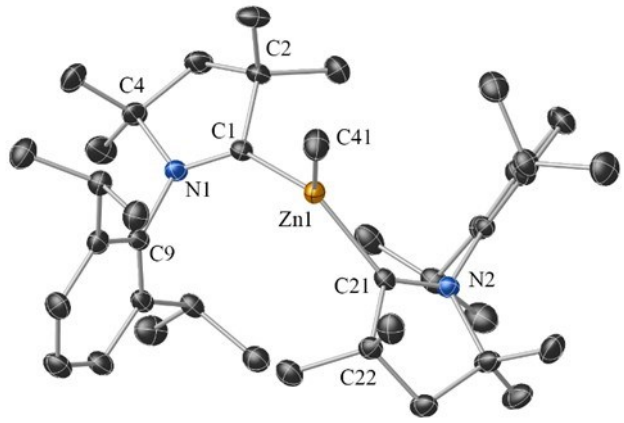

Figure 4. Molecular structure of cation [(CAAC)$_2$Zn–Me]$^+$ (**6**$^+$, ORTEP plot with thermal ellipsoids shown at the 30% probability level). Hydrogen atoms are omitted and selected atoms are labelled for clarity. Selected distances (Å) and angles (°): Zn(1)–C(1) = 2.052(3), Zn(1)-C(21) = 2.045(3) Å, Zn(1)–C(41) = 2.003(3), C(1)–Zn–C(21) = 125.0(1).

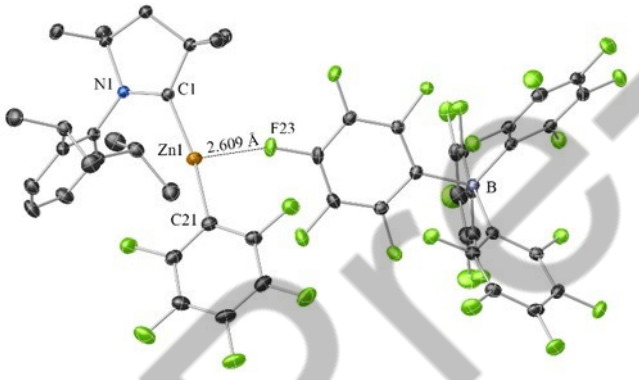

Figure 5. Molecular structure of ion pair [(CAAC)Zn–C_6F_5][$B(C_6F_5)_4$] ([**7**][$B(C_6F_5)_4$], ORTEP plot with thermal ellipsoids shown at the 30% probability level). Hydrogen atoms are omitted and selected atoms are labelled for clarity. Selected distances (Å) and angles (°): Zn–C(1) = 1.971(3), Zn–C(21) = 1.935(3), Zn···F(23) = 2.609(2), C(1)–Zn–C(21) = 169.3(1).

Cation (CAAC)Zn–Me$^+$ (**5**$^+$) cleanly reacts with $B(C_6F_5)_3$ to quantitatively yield the more Lewis acidic cation (CAAC)Zn–$C_6F_5^+$ (**7**$^+$, Scheme 3), through a Me/C_6F_5 ligand exchange reaction. Cation **7**$^+$, isolated as a $B(C_6F_5)_4^-$ salt (50% yield), crystallizes as **7**$^+$/$B(C_6F_5)_4^-$ ions in close contact (Figure 5) with, for instance, a rather short Zn···F(23) (2.609(2) Å] well below the sum of van der Waals radii of F and Zn. The structural and bonding parameters are overall very similar to those of [**5**][$B(C_6F_5)_4$]. DOSY NMR data for [**7**][$B(C_6F_5)_4$] support the persistence of ion pairs in solution (C_6D_5Br, room temperature) with an estimated hydrodynamic volume (1343 Å^3, Figure S25, SI) nearly identical to the evaluated volume of [**7**][$B(C_6F_5)_4$] in the solid state (1325 Å^3, Figure S26, SI).[21] In addition, the proximity of **7**$^+$ and $B(C_6F_5)_4^-$ ions in solution is further supported by 2D ^{1}H-^{19}F HOESY data (Figure S27, SI). Noticeably, cation **7**$^+$, stable for days in CD_2Cl_2 at room temperature, is thus significantly more robust than its Zn–Me$^+$ analogue.

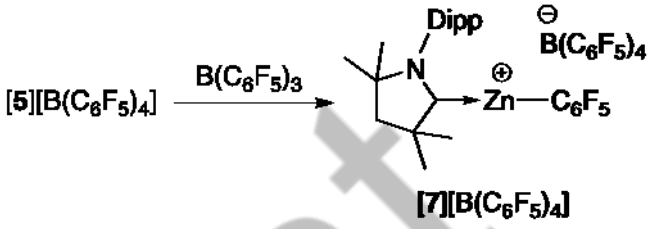

Scheme 3. Synthesis of (CAAC)Zn–$C_6F_5^+$ as a $B(C_6F_5)_4^-$ salt [**7**][$B(C_6F_5)_4$].

Electronic structure and Lewis acidity assessment of cations 5$^+$ and 7$^+$. The electronic features of Lewis acidic cations **5**$^+$ and **7**$^+$ were estimated through DFT calculations (B3LYP/6-31+G**/GD3). In particular, the LUMO energy level of such Lewis acids may correlate to their reactivity/electrophilicity.[22,23,24] The LUMO of cations **5**$^+$ and **7**$^+$ (-5.53 and -5.86 eV, respectively; Figure 6) features a π-bonding interaction between the C_{CAAC} atom and one of the empty *p* orbitals on Zn(II) and is significantly lower in energy than that of the NHC analogue (IDipp)Zn–R$^+$ (-4.61 and -4.91 eV for R = Me, C_6F_5, respectively).[14b] The latter reflects the stronger π accepting character of CAAC (*vs.* NHC ligand) and should enhance the reactivity of such cations provided orbital control is at play to some extent in these systems. NBO analysis of cations **5**$^+$ and **7**$^+$ (Table S2, SI) are consistent with Zn–C_{CAAC} and Zn–R bonds being covalent with a strong ionic character (Wiberg indexes ranging from 0.38 to 0.64). The charge at Zn(II) (1.18 for **5**$^+$ and 1.20 for **7**$^+$) is similar to those in NHC-Zn analogues.

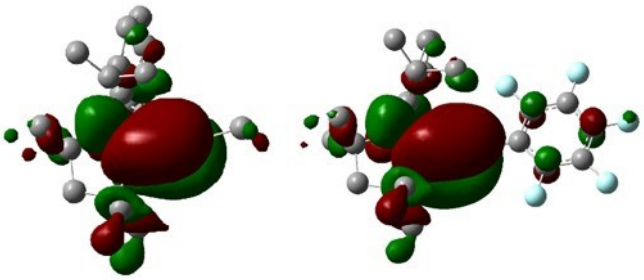

Figure 6. DFT-computed (BLYP/6-31+G**) LUMO of **5**$^+$ (left, -5.53 eV) and **7**$^+$ (right, -5.86 eV).

The Lewis acidity of cations **5**$^+$ and **7**$^+$ was experimentally assessed using the Gutmann-Beckett method, which uses the ^{31}P NMR chemical shift difference between coordinated and free

$Et_3P{=}O$ to quantify Lewis acidity.[25] According to these measurements, the Lewis acidity of the Zn–Me cation **5**$^+$ is higher than that of (IDipp)Zn–Me$^+$, comparable to $Zn(C_6F_5)_2$ but lower than that of $B(C_6F_5)_3$ [$\Delta\delta^{31}P$ (CD_2Cl_2) = 16.5, 9.5, 17.2, 26.4 ppm for **5**$^+$, (IDipp)Zn–Me$^+$, $Zn(C_6F_5)_2$ and $B(C_6F_5)_3$, respectively], albeit within the limit of validity of such a method.[26] As expected, cation **7**$^+$ is a stronger Lewis acid than **5**$^+$ and compares to $B(C_6F_5)_3$ and (IDipp)Zn–$C_6F_5^+$ [$\Delta\delta^{31}P$ (CD_2Cl_2) = 21.5, 26.4 and 24.7 ppm for **7**$^+$, $B(C_6F_5)_3$ and (IDipp)Zn–$C_6F_5^+$]. The Fluoride Affinity Ion (FIA) of cations **5**$^+$ and **7**$^+$ was also evaluated through computation (*via* a known methodology, see SI), since it may be a reliable probe to estimate the Lewis acidity of strong/hard Lewis acids.[24,27] FIA calculations agree with **5**$^+$ and **7**$^+$ being more Lewis acidic than $B(C_6F_5)_3$ [FIA = 146, 158 and 106 kcal.mol^{-1} for **5**$^+$, **7**$^+$ and $B(C_6F_5)_3$, respectively] and of comparable strength to (IDipp)Zn–Me$^+$ and (IDipp)Zn–$C_6F_5^+$, respectively.

Several recent reports on various main group heteroelement/metal electrophilic species showed that their Lewis acidity may correlate with the LUMO energy level.[22,24] However, based on our results, such correlation does not apply to the present carbene-stabilized Zn(II) cations (carbene = NHC, CAAC) since the lower lying LUMO of CAAC cations **5**$^+$ and **7**$^+$ (*vs.* NHC analogues) little affects their Lewis acidity, albeit within the limit of validity of the estimation methods.

Hydrosilylation catalysis with cation 7$^+$. Cations **5**$^+$ and **7**$^+$ were first tested as alkene and alkyne hydrosilylation to probe their ability for small molecules activation. No reaction was observed using the less Lewis acidic Zn–Me$^+$ as catalyst (**5**$^+$, mol 5%) in the presence of $HSiEt_3$ and 1-hexene under the studied conditions (CD_2Cl_2, RT, 24 h). In contrast, under identical conditions, the stronger Lewis acid **7**$^+$ cleanly and quantitatively hydrosilylates 1-hexene at room temperature to selectively afford the *anti*-Markovnikov product, triethyl(hexyl)silane (**8**, 95% conv., CD_2Cl_2, RT, 28 h, Scheme 4), as deduced from ^{1}H NMR data and comparison with literature data. The absence of any hydrosilylation activity with cation **5**$^+$ and the fact that cation **7**$^+$ retains its integrity as the catalysis proceeds (as ^{1}H NMR monitored) strongly suggest a Lewis-acid-type catalysis as observed with borane catalysts.[28] ^{1}H NMR monitoring experiments (CD_2Cl_2, RT) of 1/1 mixtures of **7**$^+$/$HSiEt_3$, **7**$^+$/1-hexene and a 1/1/1 **7**$^+$/$HSiEt_3$/1-hexene mixture showed no observable interaction between **7**$^+$ and the substrates prior to product formation. Cation **7**$^+$ (mol 5%) also mediates alkyne hydrosilylation catalysis with the fast consumption of a 1/1 $HSiEt_3$/1-octyne mixture to afford alkenylsilane (*Z*)-triethyl(oct-1-en-1-yl)silane (**9**, 40% conv., CD_2Cl_2, RT, 1 h, Scheme 4) along with uncharacterized hydrosilylation products. Cation **7**$^+$ thus lies among the rare Zn-based catalysts able to mediate alkene/alkyne hydrosilylation catalysis.

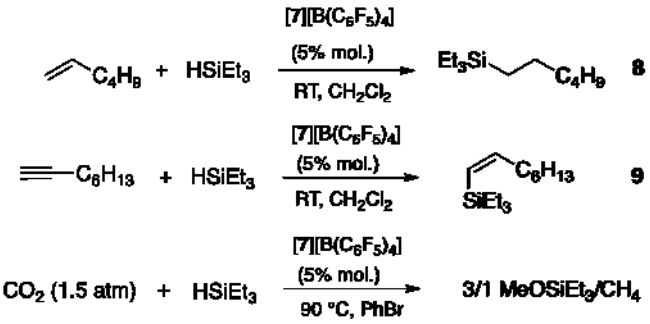

Scheme 4. Hydrosilylation reactions catalyzed by [**7**][$B(C_6F_5)_4$].

Metal-catalyzed CO_2 hydrosilylation, preferably with cheap and non-toxic organometallics, is currently attracting considerable attention as an efficient route to CO_2-derived small molecules with added value such as HCO_2SiR_3, R_3SiO-CH_2-$OSiR_3$, $MeOSiR_3$ (formate-, aldehyde- and methanol-equivalent, respectively) and CH_4.[29] Only a few Zn-based catalysts for CO_2 functionalization have thus far been developed.[14,30] Cations **5**$^+$ and **7**$^+$ were thus tested as potential CO_2 functionalization catalysts. CAAC-Zn cation **5**$^+$ is unreactive towards CO_2 (1.5 atm) in the presence of $HSiEt_3$ under the studied conditions (mol 5% of **5**$^+$, C_6D_5Br, 90 °C, 24 h). In contrast, the more Lewis acidic cation **7**$^+$ catalyzes CO_2 hydrosilylation to a 3/1 $MeOSiEt_3/CH_4$ mixture (C_6D_5Br, 90 °C, complete $HSiEt_3$ consumption after 37 h) along with $Et_3SiOSiEt_3$ as a side-product. ^{1}H NMR monitoring experiments (C_6D_5Br, 90 °C) showed that cation **7**$^+$ is unreactive with CO_2 or $HSiEt_3$ on their own, exhibits no observable interaction with a 1/1 $CO_2/HSiEt_3$ mixture (prior to hydrosilylation product formation) and retains its integrity as the catalysis proceeds. A Lewis-acid-type mechanism is thus likely operative in the present Zn system, as that recently and thoroughly described in CO_2 hydrosilylation by a $B(C_6F_5)_3/Al(C_6F_5)_3$ tandem catalyst.[31]

For further insight into the CO_2 hydrosilylation mediated by cation **7**$^+$, the initial CO_2 activation/functionalization was DFT-computed (B3LYP/6-31+G**/GD3) and the calculations agree with a Lewis-acid-type mechanism. As depicted in Figure 7, the reaction is best computed through encounter complex **VII-CO$_2$** (ΔG = 11.9 kcal.mol^{-1} from isolated model cation **VII**, CO_2 and $HSiEt_3$; Figure S39, SI) and then transition state **TS-VII-CO$_2$** (ΔG = 31.8 kcal.mol^{-1}; Figure S40, SI), in which the *H*–Si hydride undergoes a nucleophilic backside attack at the Zn-coordinated CO_2 moiety. The formation of the HCO_2SiEt_3 adduct **X** (Figure S41, SI) is then strongly favored thermodynamically (ΔG = -16.4 kcal.mol^{-1}), which certainly drives the reaction to completion. The estimated energy barrier for CO_2 functionalization (ΔG = 31.8 kcal.mol^{-1}) is in line with experimental data.

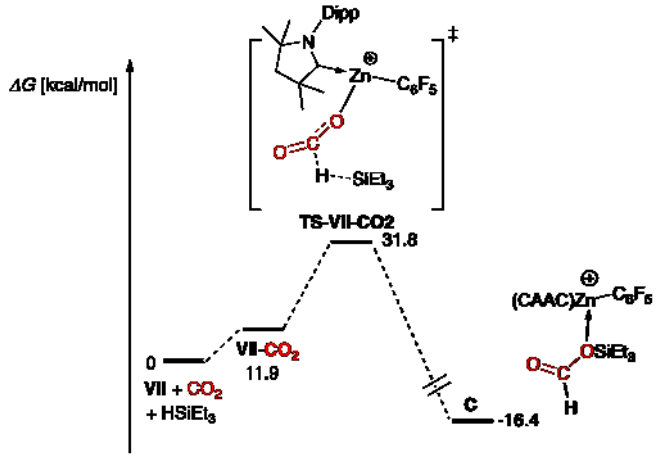

Figure 7. DFT-computed (B3LYP/6-31+G**, PhBr) reaction profile for initial CO_2 hydrosilylation catalyzed by model cation **VII**.

Summary - Conclusions

Combining Zn(II) dialkyl species such as $ZnMe_2$ with CAAC carbene may afford highly reactive/instable species but also eventually lead to robust CAAC-supported Zn(II) Lewis acids able to catalyze transformations of topical interest. Contrasting with the stability of (NHC)ZnR_2 (R = Me, Et) species, CAAC adduct of $ZnMe_2$ (**2**) is thermally unstable to readily undergo a carbene insertion into the Zn–Me bond to yield the ZnX_2-type species **3**. Such reactivity arises from the enhanced electrophilicity of the CAAC carbene atom (*vs.* that in NHC). Despite its limited stability, adduct **2** may be cleanly ionized to robust two-coordinate (CAAC)Zn–Me^+ cation (**5**$^+$) and derived into (CAAC)Zn–$C_6F_5^+$ (**7**$^+$), thus showing the suitability of CAAC for the stabilization of highly reactive oxophilic organometallics such as [Zn–Me]$^+$ and [Zn–C_6F_5]$^+$ moieties. As estimated from experimental and calculations data, cations **5**$^+$ and **7**$^+$ are highly Lewis acidic species and, as such, cation **7**$^+$ was successfully exploited in alkene, alkyne and CO_2 hydrosilylation catalysis. Despite a significantly lower lying LUMO for cation **7**$^+$ *vs.* NHC analogue (IDipp)Zn–$C_6F_5^+$, the observed reactivity and estimated Lewis acidity of both cations are comparable, clearly indicating that the reactivity of such electrophilic Zn(II) cations is solely under charge control and that the electronic differences between CAAC and NHC ligands little affect the reactivity of the derived Zn(II) cations.

Experimental Section

Material, reagents and methods. All work was performed under N_2 atmosphere using standard glove box techniques. Solvents were stored over 4 Å molecular sieves and were freshly distilled under argon from sodium-benzophenone or CaH_2, or they were dispensed from a commercial solvent purification system. Deuterated solvents were used as received and stored over 4 Å molecular sieves. NMR spectra were recorded on Bruker Avance I - 300 MHz, Bruker Avance III - 400 MHz, Bruker Avance II - 500 MHz and Bruker Avance III - 600 MHz spectrometers. NMR chemical shift values were determined relative to the residual protons in toluene-d^8, C_6D_6 and C_6D_5Br as internal reference for ^{1}H (δ of the most upfield signal = 2.08, 7.16, 6.95 ppm) and $^{13}C\{^1H\}$ (δ of the most downfield signal = 137.48, 128.06, 130.89 ppm). $HSiEt_3$, Et_3PO, 1-hexene and 1-octyne were purchased from Aldrich. 1-hexene and 1-octyne were stored over molecular sieves (4 Å) for at least 24 h prior to use. $ZnMe_2$ and $[CPh_3][B(C_6F_5)_4]$ were obtained from Strem Chemicals Inc. $B(C_6F_5)_3$ was obtained from TCI Europe and recrystallized from cold pentane prior to use. Cyclic (alkyl)(amino)carbene (CAAC) **1** was prepared according to a literature procedure.[3a]

Generation of adduct (CAAC)$ZnMe_2$ (2). *In toluene*: To a -35 °C solution of $ZnMe_2$ (13.4 mg, 11 µL, 140 µmol) in deuterated toluene (0.25 mL) was added dropwise a -35 °C solution of CAAC (40 mg, 140 µmol) in deuterated toluene (0.25 mL) giving a colorless solution. The mixture was then immediately transferred in a J-Young NMR tube and a ^{1}H NMR spectrum at -80 °C was immediately recorded, showing the quantitative formation of (CAAC)$ZnMe_2$ (**2**) on the basis of ^{1}H and ^{13}C NMR data. Adduct **2** is stable in toluene at -40 °C for 12 h but decomposes fast at room temperature, precluding its isolation in a pure form. Likewise, adduct **2** is also thermally unstable in the solid state. *In pentane*: the addition of a pentane solution (5 mL) of $ZnMe_2$ (20.1 mg, 16.5 µL, 210 µmol), cooled at -40 °C, to a pentane solution of CAAC **1** (60 mg, 210 µmol), also cooled at -40 °C, resulted in the immediate precipitation of a colorless solid, presumably adduct $CAACZnMe_2$ (**2**). The collected colorless solid is however unstable under vacuum (turning into a black insoluble residue within a few minutes), thus preventing further characterization. ^{1}H NMR (600 MHz, tol-d^8, 193 K): δ (ppm) 7.06 (t, *J* = 7.8 Hz, 1H, CH-Ar), 6.85 (d, *J* = 7.8 Hz, 2H, CH-Ar), 2.70 (hept, *J* = 6.7 Hz, 2H, CH-^{i}Pr), 1.32 (s, 6H, NC(*Me*)$_2$CH$_2$C(Me)$_2$CN), 1.27 (d, *J* = 6.7 Hz, 6H, CH$_3$-^{i}Pr), 1.22 (s, 2H, NC(Me)$_2$C*H*$_2$C(Me)$_2$CN), 1.08 (d, *J* = 6.7 Hz, 6H, CH$_3$-^{i}Pr), 0.79 (s, 6H, NC(Me)$_2$CH$_2$C(*Me*)$_2$CN), -0.28 (s, 6H, ZnMe). ^{13}C NMR (150 MHz, Tol-d8, 193 K): δ (ppm) 267.6 ($C_{carbene}$–Zn), 144.9 (C-Ar), 134.2 (C-Ar), 129.6 (CH-Ar), 125.1 (CH-Ar), 81.6 (NC(Me)$_2$CH$_2$*C*(Me)$_2$CN), 55.7 (N*C*(Me)$_2$CH$_2$C(Me)$_2$CN), 48.9 (NC(Me)$_2$*C*H$_2$C(Me)$_2$CN), 28.9 (CH-^{i}Pr), 28.1 (NC(Me)$_2$CH$_2$C(*Me*)$_2$CN), 27.9 (NC(*Me*)$_2$CH$_2$C(Me)$_2$CN)), 26.6 (CH$_3$-^{i}Pr), 23.4 (CH$_3$-^{i}Pr), -3.76 (ZnMe).

NMR characterization of (CAAC-Me)Zn–Me (3). In a J-Young NMR tube, the decomposition of adduct (CAAC)$ZnMe_2$ (**2**) in deuterated toluene was monitored by variable temperature ^{1}H and ^{13}C NMR. After 1 h at room temperature, 83% of (CAAC)$ZnMe_2$ was consumed to yield (CAAC–Me)ZnMe (**3**) as the major product (72% conversion, relative to CAAC, by ^{1}H NMR). Compound **3** is instable at room temperature to decompose to organic residues **4** and **4'**(*vide infra*), which precluded the isolation of **3** in a pure form. NMR signals assignment done on the basis of 1D (1H, 13C) and 2D (HSQC, HMBC, COSY, NOESY) are consistent with the proposed formulation for **3**. ^{1}H NMR (600 MHz, Tol-d8, 233 K): δ (ppm) 7.14-7.11 (m, 2H, CH-Ar), 6.96 (dd, *J* = 5.7, 3.8 Hz, 1H, CH-Ar), 4.21 (hept, *J* = 5.9 Hz, 1H, CH-^{i}Pr), 3.54 (hept, *J* = 5.9 Hz, 1H, CH-^{i}Pr), 1.75 (d, *J* = 13.1 Hz, 1H, NC(Me)$_2$C*H*$_2$C(Me)$_2$CN), 1.54 (d, *J* = 13.1 Hz, 1H, NC(Me)$_2$C*H*$_2$C(Me)$_2$CN), 1.29 (d, *J* = 6.7 Hz, 3H, CH$_3$-^{i}Pr), 1.26 (d, *J* = 6.7 Hz, 3H, CH$_3$-^{i}Pr), 1.21 (d, *J* = 6.7 Hz, 3H, CH$_3$-^{i}Pr), 1.16 (d, *J* = 6.7 Hz, 3H, CH$_3$-^{i}Pr), 1.16 (s, 3H, NC(Me)$_2$CH$_2$C(*Me*)$_2$CN), 1.11 (s, 3H, NC(*Me*)$_2$CH$_2$C(Me)$_2$CN), 1.09 (s, 3H, NC(*Me*)$_2$CH$_2$C(Me)$_2$CN), 1.06 (s, 3H, NC(Me)$_2$CH$_2$C(*Me*)$_2$CN, 0.87 (s, 3H, C(*Me*)ZnMe), -0.23 (s, 3H, Zn*Me*). ^{13}C NMR (150 MHz, Tol-d^8, 233 K): δ (ppm) 153.96 (C-Ar), 150.23 (C-Ar), 138.1 (C-Ar), 126.81 (CH-Ar), 125.0 (CH-Ar), 124.11 (CH-Ar), 74.86 (*C*(Me)ZnMe), 60.23 (N*C*(Me)$_2$CH$_2$C(Me)$_2$CN), 58.71 (NC(Me)$_2$*C*H$_2$C(Me)$_2$CN), 31.28 (*C*H-^{i}Pr), 30.85 (NC(*Me*)$_2$CH$_2$C(Me)$_2$CN), 29.85 (NC(Me)$_2$CH$_2$C(*Me*)$_2$CN), 29.71 (NC(*Me*)$_2$CH$_2$C(Me)$_2$CN), 27.32 (CH-^{i}Pr), 26.35 (CH$_3$-^{i}Pr), 26.22 (CH$_3$-^{i}Pr), 24.19 (CH$_3$-^{i}Pr), 23.50 (CH$_3$-^{i}Pr), 22.95 (NC(Me)$_2$CH$_2$C(*Me*)$_2$CN), 19.49 (C(*Me*)ZnMe), -5.73 (ZnMe).

X-ray Crystallographic characterization of (CAAC-Me)Zn–Me (3). Adduct CAACZnMe$_2$ (**2**) was generated *in situ* as described above in pentane at -40 °C. The mother liquor was then left 1 h at room temperature and was cooled down to -35 °C for 48 h, after which colorless crystals had formed. Their analysis through X-ray crystallography confirmed the molecular structure of **3** as (CAAC-Me)Zn–Me.

Characterization of (CAAC)ZnMe$_2$ decomposition products 4, 4'. A deuterated toluene solution of (CAAC)ZnMe$_2$ (0.140 mmol) prepared as described previously was left at room temperature for two days to monitor the decomposition process by ^{1}H NMR. During this time, adduct **2** was completely consumed, leading to the formation of a Zn metal precipitate, along with CH_4, free ZnMe$_2$ and three unknown CAAC derivatives. After removal of Zn metal, the mixture was dried under vacuum to remove CH_4 and ZnMe$_2$ affording a white solid that was solubilized in pentane and passed through a silica plug to afford white crystalline solid after solvent removal under vacuum. NMR of the mixture and high-resolution mass spectrometric data allowed the identification of the two main CAAC derivatives **4** and **4'** in 63% and 31% conversion, respectively, relative to **2**. The structure and NMR assignment for **4** and **4'** are proposed on the basis of 1D (1H, 13C) and 2D (HSQC, HMBC, COSY, NOESY) NMR data and mass spectrometric analysis.

1-(2,6-diisopropylphenyl)-2,2,4,4-tetramethyl-5-methylenepyrrolidine (**4**) ^{1}H NMR (500 MHz, C_6D_6, 298 K): δ (ppm) 7.24 (dd, *J* = 7.2 Hz, 1H, CH-Ar), 7.17 (d, *J* = 7.2 Hz, 2H, CH-Ar), 3.07 (s, 1H, C=C*H*$_2$), 3.27 (hept, *J* = 6.8 Hz, 2H, CH-^{i}Pr), 3.50 (s, 1H, C=C*H*$_2$), 1.78 (s, 2H, NC(Me)$_2$C*H*$_2$C(Me)$_2$CN),1.34 (s, 6H, NC(*Me*)$_2$CH$_2$C(Me)$_2$CN), 1.28 (d, *J* = 6.8 Hz, 6H, CH$_3$-^{i}Pr), 1.27 (d, *J* = 6.8 Hz, 6H, CH$_3$-^{i}Pr), 1.11 (s, 6H, NC(Me)$_2$CH$_2$C(*Me*)$_2$CN). ^{13}C NMR (150 MHz, C_6D_6): δ (ppm) 163,84 (*C*=CH$_2$), 150.71 (C-Ar), 134.64 (C-Ar), 124.82 (CH-Ar), 70.88 (C=*C*H$_2$), 63.30 (NC(Me)$_2$CH$_2$*C*(Me)$_2$CN), 54.36 (NC(Me)$_2$*C*H$_2$C(Me)$_2$CN), 40.92 (N*C*(Me)$_2$CH$_2$C(Me)$_2$CN), 31.91 (NC(Me)$_2$CH$_2$C(*Me*)$_2$CN), 29.61 (NC(*Me*)$_2$CH$_2$C(Me)$_2$CN), 28.79 (CH-^{i}Pr), 26.82 (CH$_3$-^{i}Pr), 23.89 (CH$_3$-^{i}Pr). Ms: m/z 300.2699, 301.2726, 302.2753 (theoretical mass for the molecular peak of **4**: 300.2647).

1-(2,6-diisopropylphenyl)-5-ethylidene-2,2,4,4-tetramethylpyrrolidine (**4'**) ^{1}H NMR (500 MHz, C_6D_6, 298 K): δ (ppm) 7.20 (d, *J* = 6.0 Hz, 1H, CH-Ar), 7.17 (d, *J* = 6.0 Hz, 1H, CH-Ar), 7.11 (dd, *J* = 6.0, 6.0 Hz, 1H, CH-Ar), 4.06 (hept, *J* = 6.6 Hz, 1H, CH-^{i}Pr), 3.65 (q, *J* = 6.4 Hz, 1H, C=C(Me)*H*), 3.41 (hept, *J* = 6.9 Hz, 1H, CH-^{i}Pr), 1.80 (d, *J* = 12.7 Hz, 1H, NC(Me)$_2$C*H*$_2$C(Me)$_2$CN), 1.74 (d, *J* = 12.7 Hz, 1H, NC(Me)$_2$C*H*$_2$C(Me)$_2$CN), 1.32 (d, *J* = 6.6 Hz, 3H, CH$_3$-^{i}Pr), 1.27 (d, *J* = 6.9 Hz, 3H, CH$_3$-^{i}Pr), 1.17 (m, 6H, CH$_3$-^{i}Pr), 1.21 (s, 3H, NC(*Me*)$_2$CH$_2$C(Me)$_2$CN), 1.12 (s, 3H, NC(Me)$_2$CH$_2$C(*Me*)$_2$CN), 1.08 (s, 3H, NC(*Me*)$_2$CH$_2$C(Me)$_2$CN), 0.98 (s, 3H, NC(Me)$_2$CH$_2$C(*Me*)$_2$CN, 0.78 (d, *J* = 6.4 Hz, 3H, C=C(Me)*H*). ^{13}C NMR (150 MHz, C_6D_6): δ (ppm) 153.09 (C-Ar), 152.37 (*C*=C(Me)H), 151.97 (C-Ar), 138.0 (C-Ar), 127.1 (CH-Ar), 124.69 (CH-Ar), 124.63 (CH-Ar), 67.78 (C=*C*(Me)H), 61.10 (N*C*(Me)$_2$CH$_2$C(Me)$_2$CN), 56.87 (NC(Me)$_2$*C*H$_2$C(Me)$_2$CN), 39.38 (NC(Me)$_2$CH$_2$C(Me)$_2$*C*N), 31.10 (NC(*Me*)$_2$CH$_2$C(Me)$_2$CN), 29.56 (*C*H-^{i}Pr), 29.22 (NC(*Me*)$_2$CH$_2$C(Me)$_2$CN), 28.12 (NC(Me)$_2$CH$_2$C(*Me*)$_2$CN), 27.47 (CH-^{i}Pr), 26.37 (CH$_3$-^{i}Pr), 25.71 (CH$_3$-^{i}Pr), 24.40 (CH$_3$-^{i}Pr), 24.15 (CH$_3$-^{i}Pr), 24.06 (NC(Me)$_2$CH$_2$C(*Me*)$_2$CN), 15.50 (C=C(*Me*)H). Ms: m/z 314.2543 (theoretical mass for the molecular peak of **4'**: 314.2803).

The Zn(0) was separated by decantation, washed with pentane, dried under vacuum and characterized by powder X-ray diffraction (see Fig. S16, SI), confirming its identity.

[(CAAC)Zn–Me][B(C$_6$F$_5$)$_4$] ([5][B(C$_6$F$_5$)$_4$]). To a -35 °C solution of ZnMe$_2$ (14.08 mg, 175 µmol) in C_6H_5F (1 mL) is added dropwise a -35 °C solution of CAAC (50 mg, 175 µmol) in C_6H_5F (1 mL) giving a colorless solution that is immediately added dropwise to a room temperature dark orange C_6H_5F solution of [CPh$_3$][B(C$_6$F$_5$)$_4$] (145.4 mg, 158 µmol in 1 mL) until the mixture becomes colorless, the latter indicating that [CPh$_3$][B(C$_6$F$_5$)$_4$] has completely reacted. The solvent was then immediately removed under vacuum and the oily residue triturated with pentane (3 x 5 mL) to yield a white powder. Recrystallization in C_6H_5F/pentane at -35 °C afforded [(CAAC)Zn–Me][B(C$_6$F$_5$)$_4$] as colorless crystals (120 mg, 67% yield). ^{1}H NMR (400 MHz, C_6D_5Br, 298 K): δ 7.25 (t, *J* = 7.9 Hz, 1H, CH-Ar), 7.05 (d,*J* = 7.9 Hz, 2H, CH-Ar), 2.42 (hept, *J* = 6.8 Hz, 2H, CH-^{i}Pr), 1.72 (s, 2H, NC(Me)$_2$C*H*$_2$C(Me)$_2$CN), 1.11 (s, 6H, NC(*Me*)$_2$CH$_2$C(Me)$_2$CN), 1.10 (d, *J* = 6.8 Hz, 6H, CH$_3$-^{i}Pr), 1.05 (s, 6H, NC(Me)$_2$CH$_2$C(*Me*)$_2$CN), 0.92 (d, *J* = 6.7 Hz, 6H, CH$_3$-^{i}Pr), -0.70 (s, 3H, ZnMe) ppm. ^{19}F NMR (282 MHz, C_6D_5Br, 298 K): δ (ppm) -131.64 (bd, *o*-B(C$_6$F$_5$)$_4$), -162.06 (t, J_{FF} = 21.0 Hz, *p*-B(C$_6$F$_5$)$_4$), -165.89 (bt, *m*-B(C$_6$F$_5$)$_4$). ^{13}C NMR (150 MHz, C_6D_5Br, 298 K): δ (ppm) 231.75 (carbene), 148.44 (dm, J_{CF} = 240.9 Hz, *o*-C$_6$F$_5$), 144.23 (C-Ar), 138.30 (dm, J_{CF} = 240.2 Hz, *p*-C$_6$F$_5$), 136.38 (dm, J_{CF} = 243.0 Hz, *m*-C$_6$F$_5$), 132.62 (C$_{ipso}$), 128.63 (CH-Ar), 124.59 (CH-Ar) 84.84 (NC(Me)$_2$CH$_2$*C*(Me)$_2$CN), 52.94 (N*C*(Me)$_2$CH$_2$C(Me)$_2$CN), 48.49 (NC(Me)$_2$*C*H$_2$C(Me)$_2$CN), 28.62 (CH-^{i}Pr), 28.05 (NC(Me)$_2$CH$_2$C(*Me*)$_2$CN), 26.56 (NC(*Me*)$_2$CH$_2$C(Me)$_2$CN)), 26.30 (CH$_3$-^{i}Pr), 22.30 (CH$_3$-^{i}Pr), -7.66 (Zn*Me*) ppm. Anal. Calcd. For [(CAAC)Zn–Me][B(C$_6$F$_5$)$_4$] + 1 equiv of pentane, $C_{50}H_{46}BF_{20}NZn$: N, 1.25; C, 53.76; H 4.15. Found: N, 1.28; C, 53.65; H 4.19.

[(CAAC)$_2$Zn–Me][B(C$_6$F$_5$)$_4$] ([6][B(C$_6$F$_5$)$_4$]). To a -35 °C solution of ZnMe$_2$ (14.08 mg, 157 µmol) in PhF (1 mL) is added dropwise a -35 °C solution of CAAC (50 mg, 157 µmol) in PhF (1 mL) giving a colorless solution. A dark orange PhF solution (1 mL) of [CPh$_3$][B(C$_6$F$_5$)$_4$] (145.4 mg, 0.157 mmol) was added dropwise until the mixture remained colorless. The solvent was then immediately removed under vacuum and the oily residue triturated with pentane (3 x 5 mL) to obtain an analytically pure white powder (156 mg, 75% yield). Anal. Calcd. For [(CAAC)$_2$Zn–Me][B(C$_6$F$_5$)$_4$], $C_{65}H_{65}BF_{20}N_2Zn$: N, 2.11; C, 58.68; H, 4.92. Found: N, 1.99; C, 58.35; H 4.57. ^{1}H NMR (400 MHz, CD_2Cl_2): δ (ppm) - 0.64 (s, 3H, ZnMe), 1.07 (br, 12H, C*Me*$_2$), 1.16 (d, 12H, *i*Pr), 1.30 (d, 12H, *i*Pr), 1.36 (s, 12H, C*Me*$_2$), 1.91 (s, 4H, CH$_2$), 2.76 (sept, 4H, *i*Pr), 7.35 (d, 2H, Ar), 7.47 (t, 4H, Ar); ^{19}F NMR (282 MHz, CD_2Cl_2): δ (ppm) -168.6 (t, 2F), - 164.7 (t, 1H), -134.0 (d, 2F).

[(CAAC)Zn–C$_6$F$_5$][B(C$_6$F$_5$)$_4$] ([7][B(C$_6$F$_5$)$_4$]). To a -35 °C solution of ZnMe$_2$ (14.08 mg, 175 µmol) in C_6H_5F (1 mL) is added dropwise a -35 °C solution of CAAC (50 mg, 175 µmol) in C_6H_5F (1 mL) giving a colorless solution that is immediately added drop wise to a room temperature dark orange C_6H_5F solution of [CPh$_3$][B(C$_6$F$_5$)$_4$] (145.4 mg, 158 µmol in 1 mL) until the mixture is colorless. The mixture is then added to a solution of B(C$_6$F$_5$)$_3$ (80.7 mg, 175 µmol) in C_6H_5F (1 mL) and stirred for 24 h. The solvent was removed under vacuum and the oily residue triturated with pentane (5x5 mL) to obtain [(CAAC)Zn–C$_6$F$_5$][B(C$_6$F$_5$)$_4$] as colorless crystals after recrystallization from C_6H_5F/pentane (95 mg, 50% yield). ^{1}H NMR (400 MHz, C_6D_5Br): δ (ppm) 7.27 (t, *J* = 7.8 Hz, 1H, CH-Ar), 7.08 (d, *J* = 7.8 Hz, 2H, CH-Ar), 2.51 (hept, *J* = 6.7 Hz, 2H, CH-^{i}Pr), 1.86 (s, 2H, NC(Me)$_2$C*H*$_2$C(Me)$_2$CN), 1.28 (s, 6H, NC(*Me*)$_2$CH$_2$C(Me)$_2$CN), 1.14 (d, *J* = 6.7 Hz, 6H, CH$_3$-^{i}Pr), 1.14 (s, 6Hz, NC(Me)$_2$CH$_2$C(*Me*)$_2$CN), 1.01 (d, *J* = 6.7 Hz, 6H, CH$_3$-^{i}Pr). ^{19}F NMR (282 MHz, C_6D_5Br) δ (ppm) -117.85, -118.11 (m, *o*-ZnC$_6$F$_5$), -132.52 (bd, *o*-B(C$_6$F$_5$)$_4$), -150.02 (t, J_{FF} = 19.8 Hz, *p*-ZnC$_6$F$_5$), -158.69, -159.93 (m, *m*-ZnC$_6$F$_5$), -162.97 (t, J_{FF} = 21.0 Hz, *p*-B(C$_6$F$_5$)$_4$), -166.81 (bt, *m*-B(C$_6$F$_5$)$_4$). ^{13}C NMR (150 MHz, C_6D_5Br, 298 K): δ (ppm) 229.36 (carbene), 148.46 (dm, J_{CF} = 242.4 Hz, *o*-C$_6$F$_5$), 144.0 (C-Ar), 138.31 (dm, J_{CF} = 238.6 Hz, *p*-C$_6$F$_5$), 136.38 (dm, J_{CF} = 251.3 Hz, *m*-C$_6$F$_5$), 132.52 (C$_{ipso}$), 129.84 (CH-Ar), 123.86 (CH-Ar), 86.06 (NC(Me)$_2$CH$_2$*C*(Me)$_2$CN), 53.53 (N*C*(Me)$_2$CH$_2$C(Me)$_2$CN), 48.51 (NC(Me)$_2$*C*H$_2$C(Me)$_2$CN), 28.78 (CH-^{i}Pr), 28.22 (NC(Me)$_2$CH$_2$C(*Me*)$_2$CN), 27.35 (NC(*Me*)$_2$CH$_2$C(Me)$_2$CN)), 26.73 (CH$_3$-^{i}Pr), 22.48 (CH$_3$-^{i}Pr). Anal.

Calcd. For $C_{50}H_{31}BF_{25}NZn$: N, 1.17; C, 50.17; H 2.61. Found: N, 1.21; C, 50.26; H 2.42.

[1] a) S. P. Nolan in *N-Heterocyclic Carbenes: Effective Tools in Organometallic Synthesis* (Eds.: S. P. Nolan), Wiley-VCH, Weinheim, **2014**; b) D. Bourissou, O. Guerret, F. Gabbaï, G. Bertrand, *Chem. Rev.* **2008**, *1*, 39; c) W. A. Herrmann, *Angew. Chem. Int. Ed.* **2002**, *41*, 1290; *Angew. Chem.* **2002**, *114*, 1342; d) V. César, S. Bellemin-Laponnaz, L. H. Gade, *Chem. Soc. Rev.* **2004**, *33*, 619; e) P. de Frémont, N. Marion, S. P. Nolan, *Coord. Chem. Rev.* **2009**, *253*, 862; f) C. Fliedel, G. Schnee, T. Avilés, S. Dagorne, *Coord. Chem. Rev.* **2014**, *275*, 63; g) S. Bellemin-Laponnaz, S. Dagorne, *Chem. Rev.* **2014**, *114*, 8747; g) H. V. Huynh, *Chem. Rev.* **2018**, *118* (19), 9457; h) Peris, E. Smart, *Chem. Rev.* **2018**, *118* (19), 9988.

[2] a) V. Nesterov, D. Reiter, P. Bag, P. Frisch, R. Holzner, A. Porzelt, S. Inoue, *Chem. Rev.* **2018**, *118* (19), 9678; b) J. Cheng, L. Wang, P. Wang, L. Deng, *Chem. Rev.* **2018**, *118* (19), 9930; c) H. W. Roesky, *J. Organomet. Chem.* **2013** *730*, 57.

[3] a) V. Lavallo, Y. Canac, A. DeHope, B. Donnadieu, G. Bertrand, *Angew. Chem. Int. Ed.* **2005**, *44*, 7236; *Angew. Chem.* **2005**, *117*, 7402; b) M. Melaimi, R. Jazzar, M. Soleilhavoup, G. Bertrand, *Angew. Chem. Int. Ed.* **2017**, *56*, 10046; *Angew. Chem.* **2017**, *129*, 10180.

[4] a) S. Roy, K. C. Mondal, H. W. Roesky, *Acc. Chem. Res.* **2016**, *49* (3), 357.

[5] a) X. Zeng, G. D. Frey, R. Kinjo, B. Donnadieu, G. Bertrand, *J. Am. Chem. Soc.* **2009**, *131*, 8690; b) X. Zeng, R. Kinjo, B. Donnadieu, G. Bertrand, *Angew. Chem. Int. Ed.* **2010**, *49*, 942; *Angew. Chem.* **2010**, *122*, 954; c) B. Rao, H. Tang, X. Zeng, L. Liu, M. Melaimi, G. Bertrand, *Angew. Chem. Int. Ed.* **2015**, *54*, 14915; *Angew. Chem.* **2015**, *127*, 15128; d) U. S. D. Paul, U. Radius, *Organometallics* **2017**, *36*, 1398; e) U. S. D. Paul, U. Radius, *Eur. J. Inorg. Chem.* **2017**, *2017*, 3362.

[6] R. Kinjo, B. Donnadieu, M. A. Celik, G. Frenking, G. Bertrand, *Science* **2011**, *333*, 610.

[7] a) S. Kundu, P. P. Samuel, S. Sinhababu, A. V. Luebben, B. Dittrich, D. M. Andrada, G. Frenking, A. C. Stückl, B. Schwederski, A. Paretzki, W. Kaim, H. W. Roesky *J. Am. Chem. Soc.* **2017**, *139*, 11028; b) S. Kundu, S. Sinhababu, S. Dutta, T. Mondal, D. Koley, B. Dittrich, B. Schwederski, W. Kaim, A. C. Stückl, H. W. Roesky, *Chem. Comm.* **2017**, *53*, 10516; c) Y. Li, Y.-C. Chan, B.-X. Leong, Y. Li, E. Richards, I. Purushothaman, S. De, P. Parameswaran, C.-W. So, *Angew. Chem. Int. Ed.* **2017**, *56*, 7573; *Angew. Chem.* **2017**, *129*, 7681.

[8] O. Back, G. Kuchenbeiser, B. Donnadieu, G. Bertrand, *Angew. Chem. Int. Ed.* **2009**, *48*, 5530; *Angew. Chem.* **2009**, *121*, 5638.

[9] a) G. D. Frey, J. D. Masuda, B. Donnadieu, G. Bertrand, *Angew. Chem. Int. Ed.* **2010**, *49*, 9444; *Angew. Chem.* **2010**, *122*, 9634; b) A. F. Eichhorn, L. Kuehn, T. B. Marder, U. Radius, *Chem. Commun.* **2017**, *53*, 11694; c) H. Schneider, A. Hock, R. Bertermann, U. Radius, *Chem. Eur. J.* **2017**, *23*, 12387.

[10] R. Kinjo, B. Donnadieu, G. Bertrand, *Angew. Chem. Int. Ed.* **2011**, *50*, 5560; *Angew. Chem.* **2011**, *123*, 5674.

[11] Y. Wei, B. Rao, X. Cong, X. Zeng, *J. Am. Chem. Soc.* **2015**, *137*, 9250.

[12] a) S. Dagorne, *Synthesis* **2018**, *50*, 3662; b) S. Budagumpi, S. Endud, *Organometallics* **2013**, 32, 1537.

[13] a) P. Jochmann, D. W. Stephan, *Chem. Eur. J.* **2014**, *20*, 8370; b) O. Jacquet, X. Frogneux, C. Das Neves Gomes, T. Cantat, *Chem. Sci.* **2013**, *4*, 2127; c) C. Fliedel, D. Vila-Viçosa, M. J. Calhorda, S. Dagorne, T. Avilés, *ChemCatChem*. **2014**, *6*, 1357; d) Y. Lee, B. Li, A. H. Hoveyda, *J. Am. Chem. Soc.* **2009**, *131*, 11625; e) T. R. Jensen, L. E. Breyfogle, M. A. Hillmyer, W. B. Tolman, *Chem. Commun.* **2004**, 2504; f) G. Schnee, C. Fliedel, T. Avilés and S. Dagorne, *Eur. J. Inorg. Chem.* **2013**, 3699.

[14] a) D. Specklin, C. Fliedel, C. Gourlaouen, J.-C. Bruyere, T. Avilés, C. Boudon, L. Ruhlmann, S. Dagorne, *Chem. Eur. J.* **2017**, *23*, 5509; b) D. Specklin, F. Hild, C. Fliedel, C. Gourlaouen, L. F. Veiros, S. Dagorne, *Chem. Eur. J.* **2017**, *23*, 15908.

[15] For a comprehensive review on Zn(II) organocations, see : M. Bochmann, *Coord. Chem. Rev.* **2009**, *253*, 2000.

[16] T. Hirose, K. Kodama, in Comprehensive Organic Synthesis, 2nd edition (eds.: P. Knochel, G. A. Molander, Elsevier B. V.) Amsterdam, **2014**, Vol. 1, pp 204-266.

[17] A. P. Singh, P. P. Samuel, H. W. Roesky, M. C. Schwarzer, G. Frenking, N. S. Sidhu, B. A. Dittrich, *J. Am. Chem. Soc.* **2013**, *135*, 7324.

[18] A. Khan, W. Jadwisienczak, M. E. Kordesch, *Physica E* **2006**, *33*, 331.

[19] L. R. Collins, G. Hierlmeier, M. F. Mahon, I. M. Riddlestone, M. K. Whittlesey, *Chem. Eur. J.* **2015**, *21*, 3215.

[20] D. Tapu, D. A. Dixon, C. Roe, *Chem. Rev.* **2009**, *109*, 3385.

[21] For the method used for volume estimation of **[7]**[$B(C_6F_5)_4$] in solution, see: a) L. Allouche, A. Marqui, J.-M. Lehn, *Chem. Eur. J.* **2006**, *12*, 7520; b) N. Giuseppone, J.-L Schmitt, L. Allouche, J.-M Lehn, *Angew. Chem. Int. Ed.* **2008**, *47*, 2235; *Angew. Chem.* **2008**, *120*, 2267.

[22] H. Böhrer, N. Trapp, D. Himmel, M. Schleep, I. Krossing, *Dalton Trans.* **2015**, *44*, 7489.

[23] H. Großekappenberg, M. Reißmann, M. Schmidtmann, T. Müller, *Organometallics* **2015**, *34*, 4952.

[24] For a recent review on strong Lewis acids and their classification, see: L. Greb, *Chem. Eur. J.* **2018**, *24*, 17881.

[25] V. Gutmann, *Coord. Chem. Rev.* **1976**, *18*, 225; b) M. A. Beckett, D. S. Brassington, M. E. Light, M. B. Hursthouse, *J. Chem. Soc. Dalton Trans.* **2001**, 1768.

[26] A. R. Nödling, K. Müther, V. H. G. Rohde, G. Hilt, M. Oestreich, *Organometallics* **2014**, *33*, 302.

[27] a) K. O. Christe, D. A. Dixon, D. McLemore, W. W. Wilson, J. A. Sheehy,J. A. Boatz, *J. Fluorine Chem.* **2000**, *101*, 151; b) L. O. Meller, D. Himmel, J. Stauffer, G. Steinfeld, J. Slattery, G. Santiso-QuiÇones, V. Brecht, I. Krossing, *Angew. Chem. Int. Ed.* **2008**, *47*, 7659; *Angew. Chem.* **2008**, *120*, 7772.

[28] Recent review on hydrosilylation catalysis by boranes: M. Oestreich, J.Hermeke, J. Mohr, *Chem. Soc. Rev.* **2015**, *44*, 2202.

[29] For a recent review on metal-mediated CO_2 hydrosilylation catalysis, see: F. J. Fernández-Alvarez, L. A. Oro, *ChemCatChem* **2018**, *10*, 4783.

[30] a) W. Sattler, G. Parkin, *J. Am. Chem. Soc.* **2011**, *133*, 9708. b) W. Sattler, G. Parkin, *J. Am. Chem. Soc.* **2012**, *134*, 17462; c) M. Khandelwal, R. J. Wehmschulte, *Angew. Chem. Int. Ed.* **2012**, *51*, 7323; *Angew. Chem.* **2012**, *124*, 7435; d) A. Rit, A. Zanardi, T. P. Spaniol, L. Maron, J. Okuda, *Angew. Chem. Int. Ed.* **2014**, *53*, 13273; *Angew. Chem.* **2014**, *126*, 13489; e) M. Rauch, G. Parkin, *J. Am. Chem. Soc.* **2017**, *139*, 18162; f) M. Tüchler, L. Gärtner, S. Fischer, A. D. Boese, F. Belaj, N. C. Mösch-Zanetti, *Angew. Chem. Int. Ed.* **2018**, *57*, 6906; *Angew. Chem.* **2018**, *130*, 7022.

[31] J. Chen, L. Falivene, L. Caporaso, L. Cavallo, E. Y.-X. Chen, *J. Am. Chem. Soc.* **2016**, *138*, 5321.